Dynamics of glycolytic regulation during adaptation of Saccharomyces cerevisiae to fermentative metabolism

Brink, J. van den; Canelas, A.B.; Gulik, W.M. van; Pronk, J.T.; Heijnen, J.J.; Winde, J.H. de; Daran-Lapujade, P.

Applied and Environmental Microbiology, Sept. 2008, p. 5710–5723 Vol. 74, No. 18
0099-2240/08/$08.00+0 doi:10.1128/AEM.01121-08

Dynamics of Glycolytic Regulation during Adaptation of *Saccharomyces cerevisiae* to Fermentative Metabolism▽†

Joost van den Brink, André B. Canelas, Walter M. van Gulik, Jack T. Pronk, Joseph J. Heijnen, Johannes H. de Winde, and Pascale Daran-Lapujade*

Kluyver Centre for Genomics of Industrial Fermentation and Department of Biotechnology, Delft University of Technology, Julianalaan 67, 2628 BC Delft, The Netherlands

Received 19 May 2008/Accepted 14 July 2008

The ability of baker's yeast (*Saccharomyces cerevisiae*) to rapidly increase its glycolytic flux upon a switch from respiratory to fermentative sugar metabolism is an important characteristic for many of its multiple industrial applications. An increased glycolytic flux can be achieved by an increase in the glycolytic enzyme capacities (V_{max}) and/or by changes in the concentrations of low-molecular-weight substrates, products, and effectors. The goal of the present study was to understand the time-dependent, multilevel regulation of glycolytic enzymes during a switch from fully respiratory conditions to fully fermentative conditions. The switch from glucose-limited aerobic chemostat growth to full anaerobiosis and glucose excess resulted in rapid acceleration of fermentative metabolism. Although the capacities (V_{max}) of the glycolytic enzymes did not change until 45 min after the switch, the intracellular levels of several substrates, products, and effectors involved in the regulation of glycolysis did change substantially during the initial 45 min (e.g., there was a buildup of the phosphofructokinase activator fructose-2,6-bisphosphate). This study revealed two distinct phases in the upregulation of glycolysis upon a switch to fermentative conditions: (i) an initial phase, in which regulation occurs completely through changes in metabolite levels; and (ii) a second phase, in which regulation is achieved through a combination of changes in V_{max} and metabolite concentrations. This multilevel regulation study qualitatively explains the increase in flux through the glycolytic enzymes upon a switch of *S. cerevisiae* to fermentative conditions and provides a better understanding of the roles of different regulatory mechanisms that influence the dynamics of yeast glycolysis.

Baker's yeast (*Saccharomyces cerevisiae*) can rapidly switch between respiratory and fermentative sugar metabolism in response to changes in the availability of oxygen and fermentable sugars. This metabolic flexibility is likely to have arisen during evolution in environments where there are strong temporal and/or spatial fluctuations in sugar and oxygen levels. Upon transfer from respiratory to fermentative conditions, *S. cerevisiae* can, within a short time, tremendously increase its catabolic rates and start accumulating ethanol, as well as smaller amounts of acetate, succinate, and glycerol (50). In the natural, evolutionary context, this may have helped this organism rapidly monopolize sugars and create a hostile environment for competing microorganisms. This metabolic flexibility of *S. cerevisiae* is also an important characteristic for its multiple industrial applications. For instance, yeast biomass starved for glucose during storage has to rapidly adapt to a very high sugar concentration when it is added to bread dough or wort. Ideally, *S. cerevisiae* cells should be able to increase their CO_2 and ethanol production rates within minutes following their introduction into a fresh production medium. Upon such a transfer, the pathways responsible for ethanol and CO_2 production, i.e., glycolysis and the fermentative enzymes (which, for convenience, are referred to here as the glycolytic pathway [Fig. 1]), have to suddenly catalyze sugar conversion at much higher rates. Two different strategies can contribute to increasing the flux through an enzyme: (i) increasing the capacity of enzymes of the pathway (V_{max}) and (ii) increasing the in vivo activity of the enzymes via metabolic regulation (i.e., regulation of activities by interaction with low-molecular-weight substrates, products, and effectors) (40). For many years *S. cerevisiae* has been a paradigm for studies of glycolysis and its regulation, and several mechanisms contributing to the regulation of V_{max} and the in vivo activity of individual enzymes have been determined. For example, it has been shown that high glucose concentrations result in modification of V_{max} by transcriptional repression of *HXK1* and *ADH2* (12) and also by covalent modification of enzymes (e.g., via the phosphorylation of Pyk1, Pyk2, and Hxk2 [28]). A sudden glucose excess also results in major changes in metabolite concentrations that, in turn, affect the in vivo activity of key enzymes, such as HXK (inhibited by trehalose-6-phosphate [4]), PFK (activated by fructose-2,6-bisphosphate [3]), and PYK (activated by fructose-1,6-bisphosphate [25]).

The contributions of these various levels of regulation to the glycolytic flux have been intensively investigated using steady-state chemostat cultures of *S. cerevisiae* grown under different conditions that resulted in a wide range of in vivo glycolytic fluxes (7, 8, 33, 36, 39, 48, 49). These studies demonstrated that, in the fully adapted, steady-state cultures, regulation of the glycolytic flux occurred predominantly via metabolite regulation and/or via processes outside the glycolytic pathway, such as sugar transport. Regulation of the synthesis or degradation of glycolytic enzymes appeared to play a relatively small (although sometimes significant) role.

The strategies employed by *S. cerevisiae* to adjust its glyco-

* Corresponding author. Mailing address: Department of Biotechnology, Delft University of Technology, Julianalaan 67, 2628 BC Delft, The Netherlands. Phone: 31 15 278 99 65. Fax: 31 15 278 23 55. E-mail: p.a.s.daran-lapujade@tudelft.nl.

† Supplemental material for this article may be found at http://aem.asm.org/.

▽ Published ahead of print on 18 July 2008.

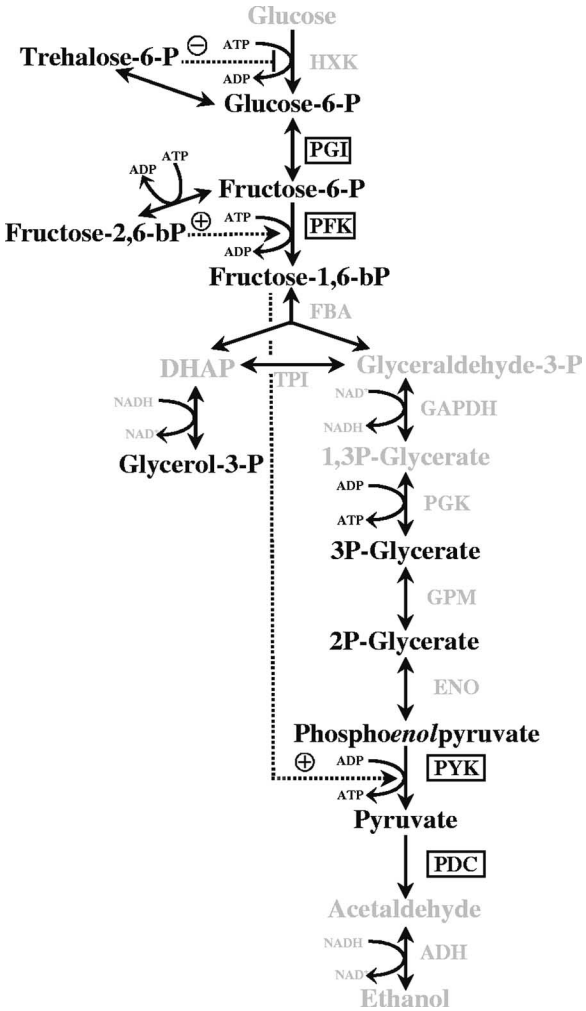

FIG. 1. Glycolytic pathway in *S. cerevisiae*. The dotted lines indicate activating (+) and inhibiting (−) actions of metabolites on enzymes. In this study, all of the glycolytic enzymes were analyzed to determine the changes in flux and capacity. Bold type indicates the metabolites measured in this study, whereas light type indicate the metabolites that could not be measured intracellularly. There is a complete metabolite data set for the glycolytic enzymes in boxes. DHAP, dihydroxyacetone phosphate.

lytic flux during dynamic responses to environmental perturbations have not been systematically investigated previously. Studies of the initial (<5-min) response to sudden relief of glucose limitation revealed widespread large changes in intracellular concentrations of metabolites (adenine nucleotides, glycolytic intermediates, and effectors), suggesting that metabolite regulation has a key role during the initial adaptation of glycolytic flux to fermentative conditions (42, 55). However, the multiple mechanisms regulating the glycolytic flux at different cellular levels have different time constants. While changes in metabolite concentrations and posttranslational modifications of proteins (e.g., phosphorylation) may occur within seconds, changes in transcript and protein levels occur much more slowly (37). In fact, the 5-min time span employed in many yeast stimulus-response studies was deliberately chosen to avoid changes in enzyme capacities that might complicate elucidation of in vivo kinetic properties (19). The regulatory events occurring after this brief first phase, which are highly relevant for understanding glycolytic regulation in natural and industrial contexts, have not been studied in detail.

Despite the large amount of knowledge gathered throughout the years about the regulation of glycolysis in yeast, we still lack a global, quantitative understanding of the contributions of the multilevel regulatory events to the regulation of the glycolytic enzymes. The only strategy that can be used to tackle this issue is to use a systems biology approach for the "glycolytic system," taking into account the regulation at multiple levels.

The goal of the present study was to understand the time-dependent regulation of glycolytic enzymes during a switch from fully respiratory conditions to fully fermentative conditions. To this end, *S. cerevisiae* cells grown in a glucose-limited aerobic chemostat with a low glycolytic flux were shifted to full anaerobiosis and glucose-excess conditions. The regulatory mechanisms were dissected by measuring the changes in metabolites, fluxes, and enzyme capacities involved in glycolysis in the 2 h following the perturbation.

MATERIALS AND METHODS

Abbreviations. HXK, hexokinase; PGI, phosphoglucose isomerase; PFK, phosphofructokinase; FBA, fructose-biphosphate aldolase; TPI, triosephosphate isomerase; GAPDH, glyceraldehyde-3-phosphate dehydrogenase; PGK, 3-phosphoglycerate kinase; GPM, phosphoglycerate mutase; ENO, enolase; PYK, pyruvate kinase; PDC, pyruvate decarboxylase; ADH, alcohol dehydrogenase; ESI-LC, electrospray ionization-liquid chromatography; MS, mass spectrometry; Γ, mass-action ratio; K_{eq}, equilibrium constant; q_{ATP}, specific ATP production rate; q_{gluc}, specific glucose consumption rate; q_{O2}, specific oxygen consumption rate.

Strain and media. The *S. cerevisiae* strain used in this study was the prototrophic haploid reference strain CEN.PK113-7D (MATa) (46). Stock cultures were grown at 30°C in shake flasks containing 100 ml of synthetic medium with 20 g of glucose per liter. The synthetic medium contained (per liter of demineralized water) 5 g of $(NH_4)_2SO_4$, 3 g of KH_2PO_4, 0.5 g of $MgSO_4 \cdot 7H_2O$, 0.15 ml of silicon antifoam (BDH), and trace elements at concentrations described by Verduyn et al. (53). After heat sterilization of the medium for 20 min at 120°C, a filter-sterilized vitamin solution (53) was added. The concentration of glucose in the reservoir medium was 7.5 g · liter^{-1}. Glucose was added to the synthetic medium after separate heat sterilization at 110°C.

Chemostat cultivation. *S. cerevisiae* CEN.PK113-7D (MATa) was grown at 30°C in 2-liter bioreactors (Applikon) with a working volume of 1.5 liters that was controlled via an electrical level sensor. Removal of effluent from the center of the culture ensured that the biomass concentrations in the effluent line differed by less than 1% from those in the culture (44). The dilution rate was set at 0.10 h^{-1}. The pH was measured online and was kept constant at 5.0 by automatic addition of 2 M KOH using an Applikon ADI 1030 biocontroller. A stirrer speed of 800 rpm and an airflow rate of 0.75 liter · min^{-1} were used to keep the dissolved oxygen concentration, as measured with an oxygen electrode, above 60% of air saturation in all chemostat cultivations performed. Steady-state samples were taken after ~10 volume changes to avoid strain adaptation due to long-term cultivation (9, 16, 24). The biomass dry weight, extracellular metabolite, dissolved oxygen, and gas profiles were constant over at least three volume changes.

Perturbation experiments. Anaerobic glucose pulse experiments were started by sparging the medium reservoir of a steady-state glucose-limited aerobic chemostat (airflow rate, 0.75 liter · min^{-1}) with pure nitrogen gas (<5 ppm O_2; Hoek-Loos, Schiedam,). Norprene tubing and butyl septa were used to minimize oxygen diffusion into the anaerobic cultures (56). Two minutes after nitrogen sparging and just before the glucose was added, the medium pump was switched off. The pulse consisted of 54 g of glucose in 60 ml demineralized water and was injected aseptically through a butyl septum. The glucose concentration immediately after the pulse was approximately 190 mM. Samples were taken 5, 10, 30, 60, and 120 min following glucose addition.

Analytical methods. The exhaust gas was cooled with a condenser connected to a cryostat set at 2°C and was dried with a Permapure dryer (Inacom Instruments) before analysis of the O_2 and CO_2 concentrations with a Rosemount NGA 2000 analyzer. The gas flow rate was determined with an Ion Science Saga digital flow meter. Acetate, ethanol, glycerol, and glucose concentrations in supernatants were determined by high-performance liquid chromatography analysis with a Bio-Rad Aminex HPX-87H column at 60°C. The column was eluted with 5 mM sulfuric acid at a flow rate of 0.6 ml · min^{-1}. Acetate was detected with a Waters 2487 dual-wavelength absorbance detector at 214 nm. Glucose, ethanol, and glycerol were detected with a Waters 2410 refractive index detector. Biomass dry weight was determined as described by Postma et al. (29), while the whole-cell protein content was determined as described by Verduyn et al. (52). Cell numbers were determined with a Coulter Counter (Multisizer II; Beckman Coulter) by using a 50-μm aperture. Specific rates of production and consumption of metabolites, expressed in mmol · g (dry weight)$^{-1}$ · h^{-1}, were calculated from measured dry weights and extracellular metabolite concentrations at 15-min intervals.

Trehalose and glycogen. Trehalose and glycogen concentrations were measured as described previously (27) using duplicate measurements for two independent replicate cultures. Glucose concentrations were determined using the UV method based on Roche kit no. 0716251.

Metabolic flux distribution. Intracellular metabolic fluxes were calculated by metabolic flux balancing using a compartmented stoichiometric model for *S. cerevisiae* grown on glucose under aerobic conditions, as described by Daran-Lapujade et al. (7). The stoichiometric models were set up and the flux balancing was performed using dedicated software (SPAD it, Nijmegen, The Netherlands). The calculated specific conversion rates and their variances for at least two independent cultures were used as input for the metabolic flux balancing procedure. The specific rates and their variances for four independent cultures (7) were used for flux balancing of the aerobic glucose-limited steady state. The q_{ATP} was calculated using $q_{ATP} = 2 \cdot q_{gluc} + 2 \cdot P/O \cdot q_{O2}$ for P/O ratios between 0.95 (54) and 1.2 (38). The ATP produced after the shift to fermentative conditions was calculated from the fluxes through the ATP-consuming and -producing glycolytic enzymes obtained from the flux balancing.

In vitro enzyme activity assays. Cell extracts were prepared by a FastPrep method (6). Enzyme activities were assayed with freshly prepared cell extracts using spectrophotometric enzyme-linked assays and a TECAN GENios Pro microtiter plate reader. All determinations were performed at 30°C and 340 nm ($\varepsilon_{NAD(P)H}$ at 340 nm = 6.33 mM^{-1}). Samples were prepared manually in microtiter plates (transparent flat-bottom Costar plates; 96 wells) in a 12-assay run using a total volume of 300 μl per well. To ensure reproducibility, all assays were performed with two concentrations of cell extracts. Each enzyme assay for the glycolytic pathway was performed as previously described (17), and data were expressed in U · mg protein^{-1} (1 U = 1 μmol · min^{-1}) Protein concentrations in cell extracts were determined by the method of Lowry et al. (23), using dried bovine serum albumin (fatty acid free; Sigma) as a standard.

Intracellular metabolites. Culture samples (1 ml) for intracellular metabolite analysis were transferred from the bioreactor with a specialized rapid sampling apparatus (22) into 5 ml of 60% (vol/vol) methanol/water at −40°C to immediately quench any metabolic activity. Samples were then processed by using the intracellular sampling processing method described previously (57) to obtain about 500 μl of intracellular metabolite solution suitable for further analysis. Glycolytic intermediates and related metabolites (glucose-6-phosphate, fructose-6-phosphate, fructose-1,6-bisphosphate, fructose-2,6-bisphosphate, 2-phosphoglycerate, 3-phosphoglycerate, phosphoenolpyruvate, glycerol-3-phosphate, and trehalose-6-phosphate) were analyzed by using ESI-LC-MS/MS as described by van Dam et al. (43), and quantification was performed by using the isotope dilution method (57). ATP, ADP, and AMP concentrations were analyzed by an ion pairing ESI-LC-MS/MS method as described by Wu et al. (57) and were also determined by the isotope dilution method (57). The energy charge (EC) (2) was calculated using equation 1:

$$EC = \frac{([ATP] + 0.5[ADP])}{([ATP] + [ADP] + [AMP])} \quad (1)$$

Kinetic rate equations. Kinetic equations describing the effects of enzyme capacity and intracellular metabolite concentrations on the activity of individual glycolytic enzymes are shown in the Appendix. The parameters used in these kinetic equations are shown in Tables 1 and 2. To obtain the sets of parameter values that best described the in vivo behavior of the enzymes, the kinetic parameters in the equations for PGI, PFK, PYK, and PDC (Michaelis-Menten constants, inhibition/activation constants, and equilibrium constants) were fitted to the in vivo metabolite and flux data. This was done using the Microsoft Excel 2003 Solver tool, with minimization of the sum of square residuals between the

TABLE 1. Parameters used for evaluation of the PGI, PYK, and PDC kinetic rate equations obtained from previous studies[a]

Enzyme	Reference	K_a		K_b		K_p		K_q		K_{eq}		K_{FbP}		L_O	n	n_H
		Concn (mM)	Fit	Concn (mM)	Fit	Concn (mM)	Fit	Concn (mM)	Fit	Concn (mM)	Fit	Concn (mM)	Fit			
PGI	41	1.4 (G6P)	5.3 (<8.1)			0.3 (F6P)	0.89 (∞)			0.31 ([F6P]/[G6P])	0.23 (>0.19, <0.30)					
PYK	41	0.14 (PEP)		0.53 (ADP)		21 (Pyr)		1.5 (ATP)		6,500 ([Pyr]/[PEP])						
	32	0.60 (PEP)	0.38 (<0.58)	0.60 (ADP)	0.37 (<7.5)			2.0 (ATP)	0.04 (<3)			3.9 (F16bP)	0.02 (<1.3)	100	4	
PDC	41	4.33 (Pyr)	0.25 (>0.13, <0.30)													1.9

[a] Two kinetic equations were tested for PYK, with and without allosteric activation by fructose-1,6-bisphosphate. The best fit to the estimated flux from the stoichiometric model is indicated in some cases (the values in parentheses indicate the asymmetric 95% confidence interval). Abbreviations: G6P, glucose-6-phosphate; PEP, phosphoenolpyruvate; Pyr, pyruvate; F6P, fructose-6-phosphate; F16bP, fructose-1,6-bisphosphate.

TABLE 2. Parameters for the PFK equation[a]

Compound	K_r (mM)	C	K (mM)	C_i
Fructose-6-phosphate	0.1	0		
ATP	0.71	3	0.65	100
Fructose-1,6-bisphosphate			0.111	0.397
Fructose-2,6-bisphosphate			6.82×10^{-4}	0.0174
AMP			0.0995	0.0845

[a] The data were obtained from the study of Teusink et al. (41).

observed in vivo flux (from the stoichiometric model) and the estimated flux (from the kinetic equation) as the objective function. The accuracy of determination of the parameter values was estimated using asymmetric 95% confidence intervals (18) (see File S1 in the supplemental material).

RESULTS

Experimental design and general physiology. *S. cerevisiae* was grown in aerobic, glucose-limited chemostat cultures at a relatively low specific growth rate (0.10 h^{-1}). These starting conditions ensured that there was full respiratory metabolism with a relatively low glucose uptake rate (ca. 1.1 $g \cdot g$ [dry weight]$^{-1} \cdot h^{-1}$) (Table 3). To allow the yeast cells to express their full fermentative potential, a concentrated glucose solution was injected into the chemostat to obtain a final concentration of 200 mM while the cultures were rapidly switched to anaerobic conditions by replacement of the incoming air by nitrogen gas. As expected, this double perturbation resulted in a rapid acceleration of fermentative metabolism (as shown by the rapid accumulation of ethanol and increasing rates of carbon dioxide production) and a large increase in the specific glucose uptake rate (Fig. 2). The specific glucose uptake rate, a key indicator of the glycolytic flux, increased for 90 min before leveling off at a value that was 13-fold higher than the glycolytic flux in the aerobic, glucose-limited chemostat culture (Fig. 2C and Table 3). The specific production rates for ethanol and CO_2, accounting for approximately 90% of the consumed carbon, exhibited the same profile as the glucose consumption rates during the 2 h after the perturbation (Fig. 2C and Table 3). The concentrations of minor metabolic products, such as acetate, lactate, pyruvate, succinate, and acetaldehyde, increased steadily but moderately, as did the glycerol concentration (Fig. 2E and F). Under anaerobic conditions, glycerol formation is generally considered to serve as a redox sink for the NADH formed during biomass formation. However, in the 2 h after the perturbation, the biomass concentration, measured as both dry weight and cell counts, increased only marginally compared to the extracellular fluxes of glucose, ethanol, and glycerol. Therefore, the biomass formation could not account for the glycerol formed (Fig. 2A). Finally, consistent with previous studies (11, 45), the sudden glucose excess triggered a swift mobilization of the reserve carbohydrates glycogen and trehalose, whose intracellular concentrations decreased to close to zero ca. 75 min after the perturbation (Fig. 2D).

All net conversion rates (i.e., the rates for glucose, O_2, CO_2, biomass, and products) calculated from the measurements obtained during the perturbation experiment were used to estimate the in vivo fluxes through the metabolic network by metabolic flux analysis, using a stoichiometric model of *S. cerevisiae* for aerobic growth on glucose (see Materials and Methods) (7). During the 2 h after the switch from aerobic to anaerobic conditions, changes may have occurred in the availability or absence of certain enzymes and thus in the stoichiometry of the metabolic network. In particular, under anaerobic conditions, the tricarboxylic acid pathway does not operate as a cycle and succinate is reductively produced via fumarate reductase (5, 13) instead of oxidatively, as it is under aerobic conditions. However, the impact of these two alternative configurations of the tricarboxylic acid pathway on glycolytic fluxes was calculated to be insignificant. The calculated fluxes through the individual glycolytic enzymes (Fig. 3) after the perturbation closely followed the glucose uptake rate (Fig. 2C). Only small fractions of the consumed glucose were channeled toward the pentose phosphate pathway and the tricarboxylic acid cycle (4 and 2% of the glucose influx, respectively) (data not shown).

The double perturbation drastically changed ATP production. When grown in aerobic glucose-limited chemostat cultures, *S. cerevisiae* displays fully respiratory glucose dissimilation, in which ATP is generated by both substrate-level and oxidative phosphorylation. This mode of dissimilation allows relatively high ATP yields, 7.2 ± 0.9 mol of ATP per mol of dissimilated glucose (assuming a P/O ratio between 0.95 [54] and 1.2 [38]). Conversely, when glucose is dissimilated by fully fermentative metabolism, such as the metabolism in the 2 h following the double perturbation, only substrate-level phosphorylation occurs, which yields at most 2 mol of ATP per mol of glucose fermented to ethanol (51). To compensate for this lower ATP yield, fermenting cells typically have higher glycolytic rates (8). However, during the first 15 min after the double perturbation, the increased glycolytic flux appeared not to be sufficient to compensate for the lower anaerobic ATP yield, as shown by the decrease in q_{ATP} compared to the preperturba-

TABLE 3. Physiological parameters for an aerobic glucose-limited chemostat culture and for 2 h after the change to anaerobic glucose-excess conditions[a]

Culture	μ	Y_{sx}	q_{gluc}	q_{O2}	q_{CO2}	q_{eth}	q_{glyc}	q_{ac}	Carbon recovery (%)
Chemostat	0.10 ± 0.01	0.50 ± 0.01	1.09 ± 0.03	2.7 ± 0.1	2.8 ± 0.1	NA[b]	NA	NA	102 ± 1
2 h after change	0.14 ± 0.00	0.07 ± 0.04	13.4 ± 1.0	NA	21.6 ± 0.9	19.6 ± 1.4	3.28 ± 0.14	0.19 ± 0.02	93 ± 7

[a] The data are the averages and standard deviations for at least three independent cultivations. Abbreviations: μ, specific growth rate determined by measurement of the dry weight; Y_{sx}, biomass yield on glucose (grams of biomass per gram of glucose consumed); q_{gluc}, millimoles of glucose consumed per gram of biomass per hour; q_{O2}, millimoles of oxygen consumed per gram of biomass per hour; q_{CO2}, millimoles of carbon dioxide produced per gram of biomass per hour; q_{eth}, millimoles of ethanol produced per gram of biomass per hour; q_{glyc}, millimoles of glycerol produced per gram of biomass per hour; q_{ac}, millimoles of acetate produced per gram of biomass per hour.

[b] NA, not applicable.

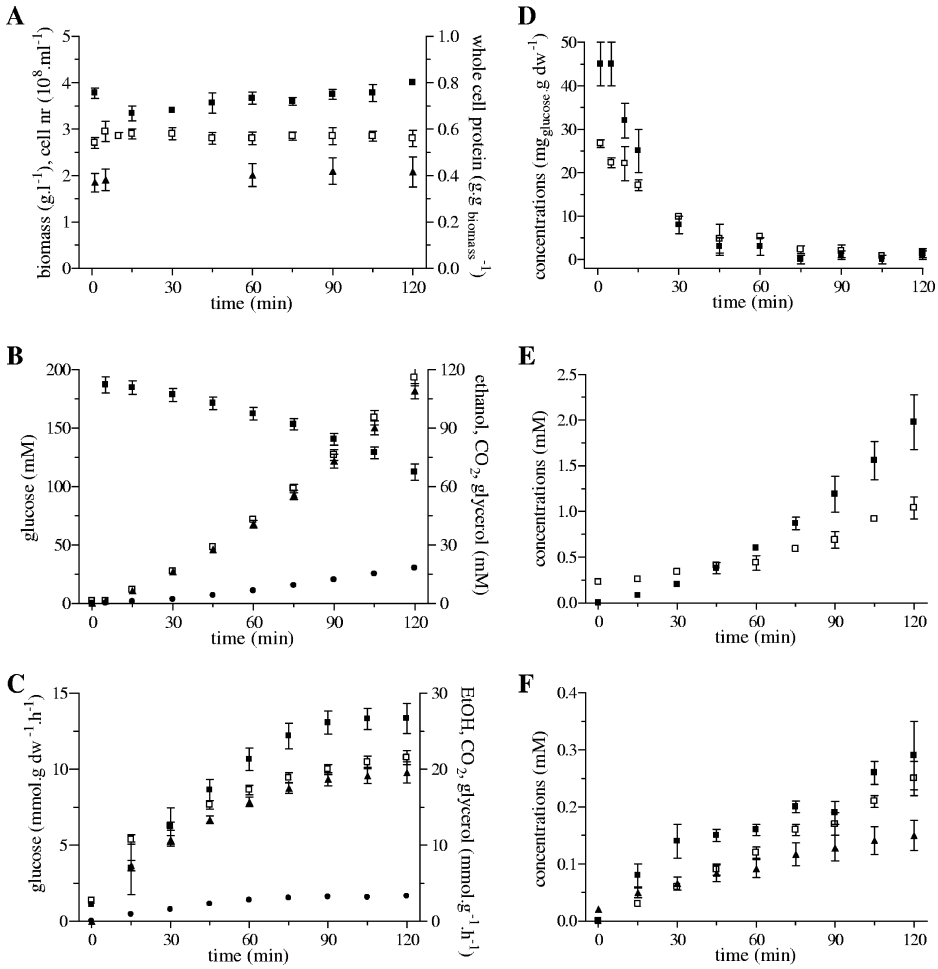

FIG. 2. General physiological response of *S. cerevisiae* after the change to fermentative conditions. (A) Symbols: ■, biomass ($g \cdot liter^{-1}$); □, whole-cell protein ($g \cdot g\ biomass^{-1}$); ▲, cell number ($cells \cdot ml^{-1}$). (B and C) Symbols: ■, □, ▲, and ●, concentrations (mM) and specific consumption rates ($mmol \cdot g^{-1} \cdot h^{-1}$) of glucose, CO_2 from the off-gas, ethanol (EtOH), and glycerol respectively. The data are data from six independent cultivations. (D) Symbols: ■ and □, intracellular concentrations of trehalose and glycogen, respectively. The results are expressed in mg glucose equivalents · g biomass^{-1}. (E) Symbols: ■ and □, concentrations (mM) of acetate and lactate, respectively. (F) Symbols: ■, □, and ▲, concentrations of extracellular pyruvate, succinate, and acetaldehyde respectively. Unless indicated otherwise, the data are the averages and standard deviations from two independent cultivations. dw, dry weight.

tion value (Fig. 4). This initial decrease in ATP production was corroborated by a rapid twofold decrease in the intracellular ATP concentration (Fig. 4). In agreement with this observation, the intracellular AMP concentration increased in the initial 15 min from 0.57 to 0.94 $\mu mol \cdot g\ (dry\ weight)^{-1}$, although the ADP concentration did not change significantly over time. The sum of the nucleotide concentrations and the calculated energy charge (2) did not change significantly during the perturbation experiment, although a transient decrease was observed in the initial phase of the experiment (Fig. 4).

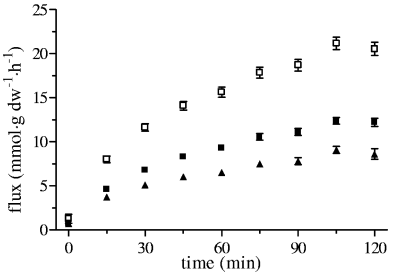

FIG. 3. Estimated in vivo fluxes through glycolysis (in $mmol \cdot g\ [dry\ weight]^{-1} \cdot h^{-1}$), as determined using a stoichiometric model (7). Symbols: ■, average flux of the upper part of glycolysis; ▲, flux of TPI; □, average flux of the lower part of glycolysis. The error bars indicate standard deviations for at least six independent culture samples.

After the initial decrease in ATP production and hence in the cellular energy level, the specific ATP production rate increased and reached values that were approximately twice the steady-state production values, while the pool of free ATP remained stable. ATP is used primarily to supply energy for biomass formation. In the absence of growth, only a relatively small part of the ATP production is necessary to sustain maintenance processes (21). Assuming a yield of 16 g (dry weight) of biomass per mol of ATP (51) and assuming that all ATP formed is used for biomass formation, the estimated growth rate should have reached 0.3 h^{-1} at 2 h after the perturbation. However, the measured growth rate after 2 h was one-half this value (ca. 0.14 h^{-1}, as determined from the dry weight mea-

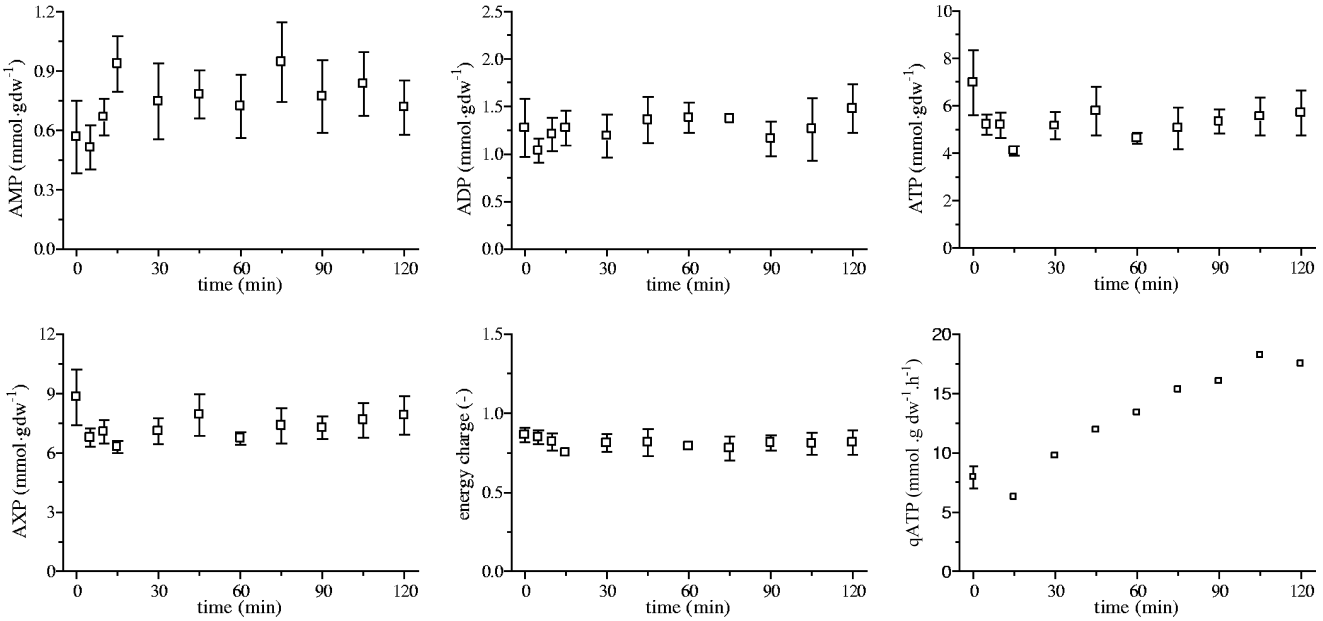

FIG. 4. Intracellular levels of adenine nucleotides (ATP, ADP, and AMP), sum of nucleotide concentrations (AXP), energy charge, and ATP production rate after the shift to anaerobic glucose-excess conditions. The error bars for the adenine concentrations indicate standard deviations for duplicate analyses of at least two independent cultures. The error bar for the steady-state value (zero time) in the q_{ATP} graph indicates the ATP production of the P/O ratio range between 0.95 and 1.2 as described in Materials and Methods. dw, dry weight.

surements), revealing that a substantial fraction of ATP generated after the shift to fermentative conditions was apparently used for processes other than biomass formation.

Changes in enzyme capacity only marginally contribute to the regulation of the carbon flux through the glycolytic steps. The shift from aerobic glucose limitation to anaerobic glucose excess triggered a strong increase in the in vivo fluxes through the glycolytic steps, resulting in fluxes that were approximately 13-fold higher at 2 h after the shift. The contribution of changes in enzyme capacity to the changes in flux can be estimated relatively easily by measuring the V_{max} of the glycolytic enzymes in in vitro assays. While such measurements do not necessarily provide an indication of the absolute in vivo capacity of the enzymes, comparison of different cultivation conditions or, as in this study, time points does allow a comparison of relative V_{max} values.

Using measurements of the V_{max} of all glycolytic enzymes (Fig. 5), it was observed that the values all remained stable during the first 45 min following the shift to fermentative conditions. After this, the enzymes HXK, PFK, TPI, PGK, and ADH maintained a constant capacity, while the capacities of PGI, FBA, GAPDH, GPM, ENO, PYK, and PDC increased significantly (Fig. 5). The time necessary for the cells to increase their enzyme capacity was not the same for all enzymes. While changes in the PDC capacity were detected after 30 min, changes in the PGI, FBA, GPM, and ENO capacities did not occur until 45 min after the shift and changes in the GAPDH and PYK capacities did not occur until 60 min after the shift. Compared to the steady-state cultures, the enzyme with the greatest change in V_{max} was PDC, whose capacity increased up to 2.5-fold. These observations indicate that increases in the glycolytic enzyme capacities could have contributed only marginally to the 13-fold increase in glycolytic fluxes and therefore indicate that the role of metabolic regulation (i.e., regulation of activities by interaction with substrates, products, and effectors) is dominant. Although, as mentioned above, in vitro enzyme activities cannot be directly translated into absolute in vivo enzyme capacities, this conclusion was consistent with the observation that the maximum capacities of all glycolytic reactions (estimated from in vitro assays), except those of PFK and PDC, were substantially higher than the actual in vivo flux channeled by these reactions (data not shown). The discrepancy between in vitro V_{max} activities and in vivo fluxes for PFK can be explained by the notorious sensitivity of this enzyme to many effectors, especially to the activator fructose-2,6-bisphosphate and the inhibitor ATP (3). The discrepancy observed for PDC was more unexpected, since this enzyme is known to be regulated by its substrate pyruvate and the phosphate concentration in the cell, but no other allosteric effectors have been reported.

Intracellular metabolites strongly influence regulation of the glycolytic flux. Since the relatively small changes in the V_{max} of the glycolytic enzymes suggested that metabolic regulation makes a major contribution to the postperturbation increase in the glycolytic flux, intracellular concentrations of glycolytic intermediates and effectors were measured (Fig. 1). Unfortunately, the intracellular concentrations of some relevant intermediates (e.g., intracellular glucose and acetaldehyde, dihydroxyacetone phosphate, glyceraldehyde-3-phosphate, glycerate 1,3-bisphosphate) could not be adequately determined. However, a complete metabolite data set was obtained for 4 of the 12 glycolytic enzymes (Fig. 6).

The first step in glycolysis, the phosphorylation of glucose, is catalyzed by three isoenzymes, glucokinase (Glk1), hexokinase 1 (Hxk1), and hexokinase 2 (Hxk2). These three isoenzymes have different characteristics; for example, they differ with re-

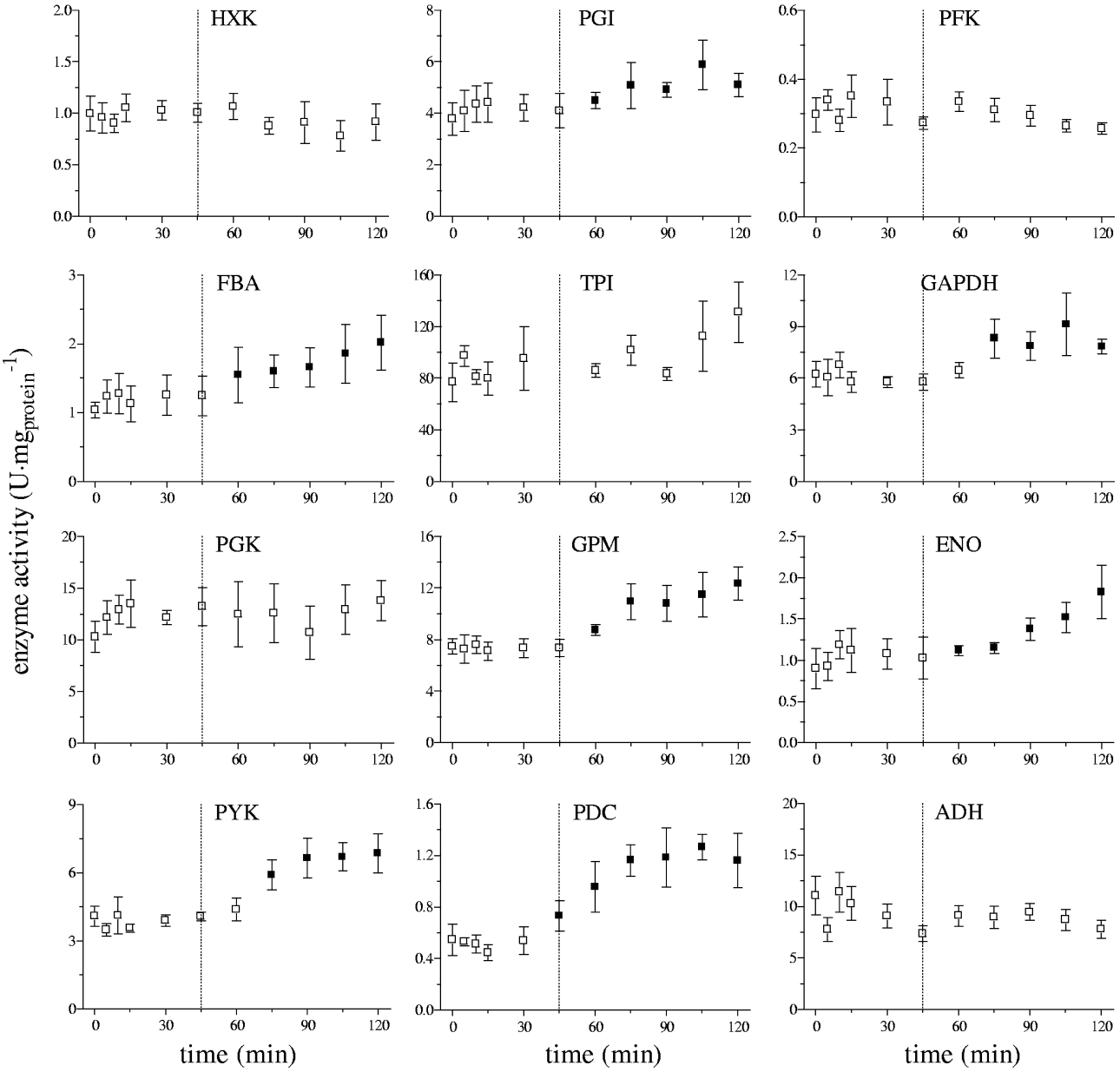

FIG. 5. Glycolytic enzyme activities after the change to anaerobic glucose-excess conditions, as determined by in vitro assays with cell extracts. Open squares indicate nonsignificant changes in in vitro enzyme activities, whereas closed squares indicate significantly changed activities ($P < 0.05$, standard Student t test compared to time zero). In vitro enzyme activities were expressed in micromoles per milligram of protein per minute. The data are data from at least four measurements for two independent cultures.

spect to the regulation of expression by the glucose concentration and the modulation of enzyme activity by different effectors. More precisely, while *HXK1* and *GLK1* are repressed by high glucose concentrations, *HXK2* is highly expressed in *S. cerevisiae* under these conditions (Fig. 7) (45). The activity of the HXKs, mainly Hxk2, is inhibited by trehalose-6-phosphate (4). The trehalose-6-phosphate concentration drastically changed during the perturbation experiment (Fig. 8), and although we did not observe changes in the V_{max} of HXK in the double-perturbation experiment, it can be reasonably assumed, taking into account the observed changes in expression levels of the isoenzymes, that the levels of Hxk1 and Hxk2 also changed following glucose addition. For this reason and because the intracellular glucose concentration was not measured, accurate prediction of the regulation of the flux through HXK was not possible.

The second step in glycolysis, catalyzed by PGI, is not known to be sensitive to allosteric effectors or cofactors and is therefore regulated mainly by changes in substrate and product concentrations. In the glucose-limited steady-state cultures, the mass-action ratio was similar to the equilibrium constant (Table 1), indicating a near-equilibrium situation. However, in the 45 min following the shift to fermentative conditions, the mass-action ratio decreased (from 0.2 to 0.1) (Fig. 6) and

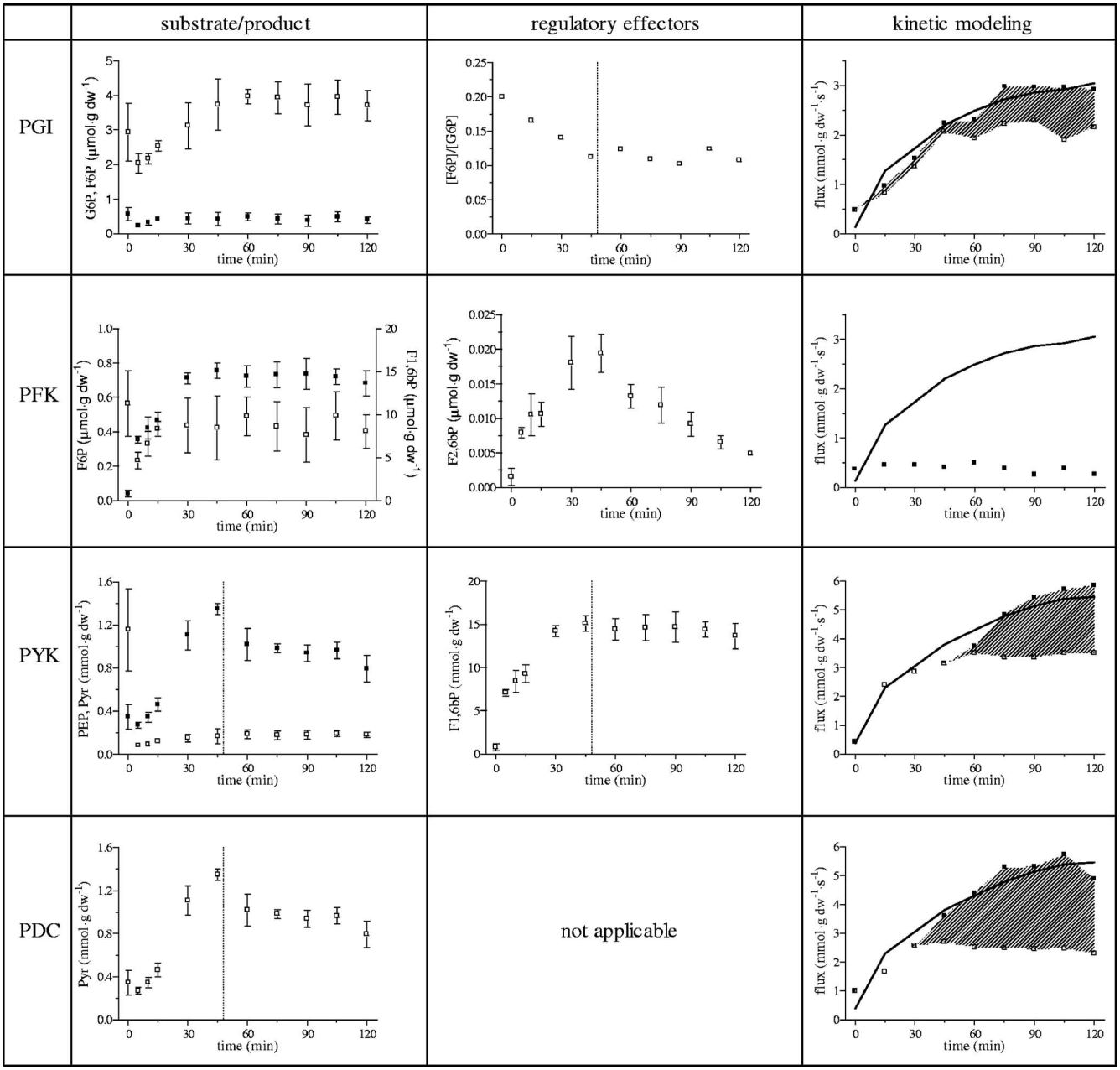

FIG. 6. Intracellular levels of substrates and products, regulatory effectors (mass-action ratio and concentrations of allosteric effectors) and flux predictions from kinetic models for four glycolytic enzymes (PGI, PFK, PYK, and PDC) after the change to anaerobic glucose-excess conditions. In the substrate/product graphs, data for glucose-6-phosphate (G6P) (□) and fructose-6-phosphate (F6P) (■) are shown for PGI, data for fructose-6-phosphate (□) and fructose-1,6-bisphosphate (F1,6bP) (■) are shown for PFK, data for phosphoenolpyruvate (PEP) (□) and pyruvate (Pyr) (■) are shown for PYK, and the bottom graph shows the data for pyruvate for PDC. The error bars indicate the mean errors for at least two independent culture samples. For the regulatory effector graphs, the mass-action ratio ([F6P]/[G6P]) is shown for PGI, the concentration of the activator fructose-2,6-bisphosphate (F2,6bP) is shown for PFK, and the concentration of the activator fructose-1,6-bisphosphate is shown for PYK. The error bars indicate the mean errors for at least two independent culture samples. For the kinetic modeling graphs, the line indicates the flux determined by stoichiometric estimation, and the filled squares indicate the predicted flux determined by kinetic modeling (41), using the best-fit parameters (Tables 1 and 2). The open squares show the predicted flux for the models with a constant enzyme capacity, while the shaded area shows the difference between the predicted fluxes with and without changing enzyme capacity. dw, dry weight.

stabilized at a twofold-lower value. This decrease in the mass-action ratio indicated that there was substantial displacement from near-equilibrium conditions (calculated from Γ/K_{eq}) from 0.67 to 0.35, which had a great effect on in vivo PGI activity (see below).

The in vivo activity of the enzyme PFK, which catalyzes an irreversible reaction, is notoriously sensitive to various metabolites, and the effects of the activators ADP, AMP, and fructose-2,6-bisphosphate and the inhibitor ATP have been described best. The concentrations of the activators AMP and

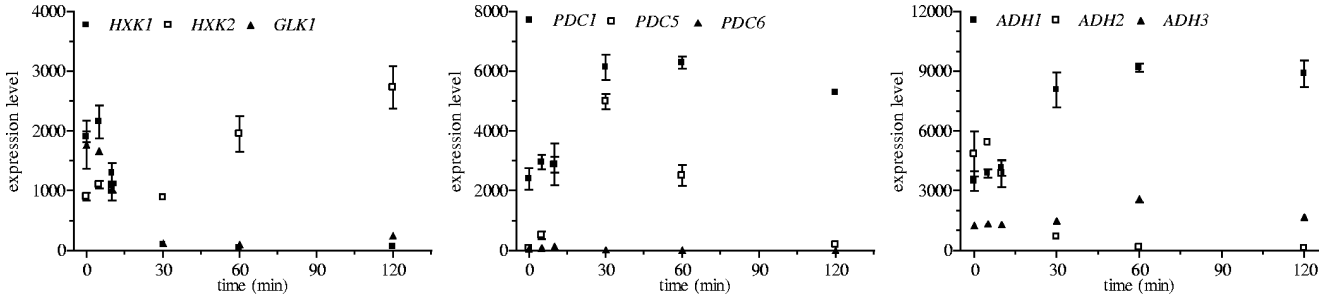

FIG. 7. Transcriptional responses of HXK, PDC, and ADH after the change to anaerobic glucose-excess conditions (45). The error bars indicate the mean errors for at least two independent culture samples.

fructose-2,6-bisphosphate increased after the double perturbation (Fig. 4 and 6). While the AMP concentration became stable after 15 min, the fructose-2,6-bisphosphate concentration kept increasing until 45 min after the perturbation and then decreased. Conversely, the concentration of the inhibitor ATP decreased after the perturbation, but, similar to the results for AMP, stabilized after 15 min (Fig. 4). These modifications in metabolite concentrations are in agreement with the acceleration of the flux channeled through PFK after the perturbation.

Several intermediates involved in the reactions between fructose-1,6-bisphosphate and phosphoenolpyruvate could not be quantified (Fig. 1). Therefore, the six consecutive reactions (the reactions catalyzed by FBA, TPI, GAPDH, PGK, GPM, and ENO) could not be fully analyzed in terms of their metabolic regulation. For two of these enzymes, GAPDH and PGK, cofactors are responsible for regulation of the in vivo activity (namely, ADP/ATP for PGK and NADH/NAD for GAPDH). The great difference in the observed responses to the double perturbation of fructose-1,6-bisphosphate (building up until 45 min and reaching a new steady state [Fig. 6]) and phosphoglycerate (strongly decreasing during the first 5 min [Fig. 8]) suggests that the cytosolic redox status has an important role in the regulation of the flux in these six glycolytic steps. Indeed, according to previous observations during a glucose pulse experiment (6), the NADH/NAD ratio was expected to increase after the double perturbation. This assumption was supported by the sudden increase in the glycerol-3-phosphate level (Fig. 8), which is known to be responsive to redox stress (26). The glycerol-3-phosphate concentration slowly decreased during the following 2 h, suggesting that the NADH/NAD balance was restored.

The next step in glycolysis is catalyzed by PYK. The concentration of the PYK substrate, phosphoenolpyruvate, decreased within the first 5 min after the shift, and the product, pyruvate, accumulated during the first 45 min (Fig. 6). However, the main allosteric regulator for the flux through PYK is a metabolite from the upper part of glycolysis, fructose-1,6-bisphosphate. The concentration of fructose-1,6-bisphosphate increased greatly in the first 5 min after the shift, strongly stimulating the PYK flux (see below).

After pyruvate, the carbon flux may be diverted into different directions. During aerobic glucose-limited growth, pyruvate is converted mainly via the mitochondrial pyruvate dehydrogenase complex, and only a small, assimilatory flux through PDC is required for synthesis of cytosolic acetyl coenzyme A (10). The flux through PDC immediately increased after the shift to anaerobic glucose-excess conditions, as reflected by ethanol production within 5 min. The most probable cause of this sudden increase in the PDC flux was a buildup of intracellular pyruvate. However, the pyruvate concentration started to increase only after 10 min, and there was up to a 3.5-fold increase after 45 min (Fig. 6). This indicates that regulation of PDC cannot be solely due to an increased pyruvate concentration and hence that other regulatory mechanisms must affect the flux through PDC.

The concentrations of the metabolites known to be involved in the in vivo regulation of ethanol production through ADH, acetaldehyde and ethanol, could not be measured intracellularly. A variety of ADH isoenzymes occur in *S. cerevisiae*, and

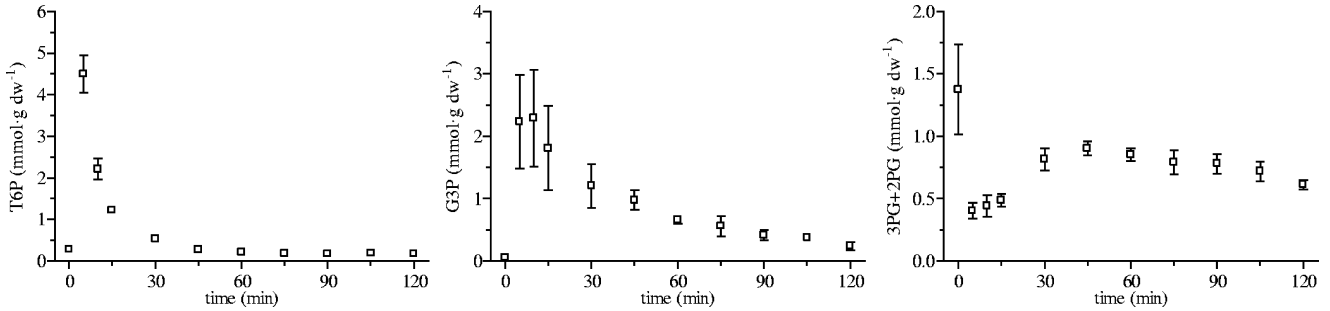

FIG. 8. Intracellular concentrations of trehalose-6-phosphate (T6P), glycerol-3-phosphate (G3P), and 3-phosphoglycerate plus 2-phosphoglycerate (3PG+2PG) after the change to anaerobic glucose-excess conditions. The error bars indicate the mean errors for at least two independent culture samples. dw, dry weight.

alcohol dehydrogenase 1 (Adh1) and alcohol dehydrogenase 2 (Adh2) are the main isoenzymes. Transcription of *ADH1* and transcription of *ADH2* respond differently to changes in the glucose concentration (Fig. 7). Although the in vitro V_{max} of ADH appeared to be stable throughout the double-perturbation experiment (Fig. 5), transcript analyses showed that *ADH1* was highly expressed after a shift to anaerobic, glucose-excess conditions, while *ADH2* was repressed (Fig. 7) (45).

Kinetic models for glycolytic enzymes only partially explain the observed flux changes. To investigate whether current kinetic models for glycolytic enzymes allow prediction of the in vivo activity of the four enzymes (PGI, PFK, PYK, and PDC) for which a complete metabolite data set was obtained, metabolite and V_{max} data were used as input for previously published kinetic equations. The main source of equations was an advanced kinetic model for yeast glycolysis (41) (see Materials and Methods). Key kinetic parameters (e.g., equilibrium constants and Michaelis-Menten constants for substrate and products) were derived from previous studies (Tables 1 and 2).

One-substrate, one-product reversible Michaelis-Menten kinetics (31) for PGI successfully predicted an increase in the metabolic flux through PGI during the double perturbation. However, the intensity of the response was stronger than the experimental observations, and the predicted flux exceeded the observed flux by about twofold (data not shown). The prediction for the flux could be improved by fitting the kinetic parameters to the experimental data, indicating that the equation format used was appropriate but that the values for in vitro-determined parameters were not appropriate. Sensitivity analysis indicated that the experimental data did not allow precise determination of the in vivo kinetic parameters (Table 1). A wide range of values for both K_ms (fructose-6-phosphate and glucose-6-phosphate) can explain the data within the 95% confidence interval, and any K_{eq} value between 0.19 and 0.30 can fit the data sufficiently well. Still, the predicted fluxes through PGI could match the calculated flux best when the equilibrium constant was decreased (Table 1). The equilibrium constant was even closer to the mass-action ratio under steady-state conditions (Γ/K_{eq} ratio, 0.8), confirming the important role of displacement from near-equilibrium for the regulation of reversible enzymes in glycolysis. In the first 45 min after the fermentative shift, the enzyme activity remained constant, indicating that the changes in flux through PGI were regulated solely by changes in the metabolite concentration (i.e., mass-action ratio). This scenario changed later, as enzyme activities increased (~1.5-fold) and substantially contributed to the flux regulation. This contribution is shown in Fig. 6, which shows the gap between flux predictions including and excluding changes in enzyme capacity. When a constant V_{max} for PGI during the 2 h following the double perturbation was considered, the predicted flux stabilized after 45 min. Flux regulation through PGI could, therefore, be divided into two phases: an initial phase (until ca. 45 min), during which changes in glycolytic fluxes were regulated mainly by changes in the mass-action ratio, and a second phase, during which fluxes through PGI were regulated by changes in V_{max}.

The V_{max} capacity of PFK remained constant after the perturbation, indicating that the flux through this enzyme was regulated solely by modulation of its in vivo activity by metabolites. The major activators ADP, AMP, and fructose-2,6-bisphosphate and the inhibitor ATP were included in a previously published kinetic equation (41) and measured in the present study (Fig. 4 and 6). The observed initial changes in metabolite concentrations were in agreement with the acceleration of the flux channeled through PFK. However, after 45 min, the concentration of the important activator fructose-2,6-bisphosphate decreased, and, using the experimentally estimated V_{max} and metabolite concentrations as input in the kinetic equation for PFK (41), we could not explain the further increase in the flux through PFK (Fig. 6). No improvement of the prediction was obtained when we attempted to fit the parameters to the measured metabolite concentrations. The current model for PFK, therefore, does not accurately reflect the kinetic mechanisms involved in the in vivo metabolic regulation of this enzyme and suggests a regulation of PFK by other, as-yet-unknown effectors.

The flux through PYK, which is known to be allosterically activated by fructose-1,6-bisphosphate, could be satisfactorily predicted only when this metabolite was added to the model (32, 41). Teusink et al. (41) did not consider the effect of this activator since under their experimental conditions, its concentration was far greater than the reported saturation concentration (0.5 mM). In our study, therefore, the kinetic equation of these authors for PYK failed to predict the in vivo activity at steady state since the fructose-1,6-bisphosphate concentration was less than 0.5 mM. Including the activation by fructose-1,6-bisphosphate in the model resulted in a reasonably good prediction of the flux profile through PYK, although lower K_ms for fructose-1,6-bisphosphate and ATP were required for a good fit (Table 1). Again, a sensitivity analysis showed that our data did not enable precise estimation of these in vivo kinetic parameters (Table 1). Approximately 60 min after the perturbation, changes in PYK capacity contributed to the increase in its in vivo activity (Fig. 6).

PDC exhibits cooperative kinetics with respect to its substrate, pyruvate (15). A previously proposed kinetic equation (41) and our metabolite and enzyme data could not predict the flux increase through PDC after the perturbation. Only by drastically decreasing the K_m of PDC for pyruvate could the flux be predicted satisfactorily (0.13 mM $< K_m <$ 0.30 mM) (Table 1), and the value is an order of magnitude lower than previously described values. Such a low K_m for pyruvate seems unlikely, as it would contradict current knowledge concerning the regulation of carbon fluxes at the pyruvate branch point (30). Furthermore, the measured V_{max} values could not explain the in vivo flux through PDC. At least part of these unexplainable findings may be due to differential expression of the three PDC isoenzymes (Pdc1, Pdc5, and Pdc6) during the double perturbation. Although enzyme assays cannot discriminate between these isoenzymes, the transcript level of *PDC5* was initially highly upregulated (70-fold), while *PDC1* expression increased only 2.5-fold and *PDC6* was barely expressed (Fig. 7).

DISCUSSION

Increased synthesis of glycolytic enzymes has a minor role in the fermentative response of *S. cerevisiae*. Sugar metabolism in *S. cerevisiae* can rapidly switch from respiration to fermentation. This switch is accompanied by a large increase in the in vivo glycolytic flux. In the present study, a shift from fully

respiratory metabolism to fully fermentative metabolism caused the glycolytic flux to increase eightfold within 45 min. As the capacities of the glycolytic enzymes (V_{max}), estimated using in vitro enzyme activity assays, did not increase during this initial period, the increase in the glycolytic flux must have been caused by changes in the in vivo activity of the glycolytic enzymes via metabolic regulation (i.e., regulation of activities by interaction with low-molecular-weight substrates, products, and effectors).

During prolonged incubation (up to 2 h) under anaerobic, glucose-excess conditions, effects at the level of enzyme induction were also observed. The contributions of enzyme induction differed among the glycolytic enzymes. Some enzyme capacities remained stable (HXK, PFK, PGK, and ADH), while others changed at ca. 45 min after the fermentative shift (PGI, FBA, GAPDH, GPM, ENO, PYK, and PDC). In contrast to the kinases of the upper part of glycolysis, the enzymes of the lower part of glycolysis showed increased enzyme capacity in the second phase after the shift to fermentative conditions. A difference in the glycolytic capacities was also found in a comparison of aerobic ("low" flux) and anaerobic ("high" flux) steady-state glucose-limited cultures (8). Apparently, a new balance of the glycolytic enzyme capacities is established, enabling a higher glycolytic flux and/or homeostasis of glycolytic metabolite levels under fermentative conditions.

The well-documented ability of *S. cerevisiae* to rapidly increase its glycolytic flux (47, 50) without a need for enzyme synthesis (48) allows fast adaptation to environmental conditions that affect central carbon metabolism, such as weak acid stress (20) and temperature changes (39). In the latter case, it has recently been proposed that the apparent "overcapacity" of glycolysis that is often observed when *S. cerevisiae* is grown at standard laboratory growth temperatures may reflect an evolutionary adaptation to diurnal temperature cycling in the natural environments of this yeast (39).

The energy level influences the induction of enzymatic capacity in glycolysis. The specific glucose consumption rate increased more than 12-fold during the 2 h after the switch to fermentative conditions. However, the rate of ATP production decreased during the first 15 min, as a result of the reduced ATP yield under fully fermentative conditions. This initial "energy crisis" may have contributed to the long delay that was observed before induction of glycolytic enzyme synthesis became evident. In *S. cerevisiae*, enzyme synthesis (transcription and translation) can take place on a time scale of a few minutes (1). In the present study, increased levels of glycolytic enzymes were observed only after ca. 45 min, although the majority of the relevant transcripts were fully induced after 10 min (45). This implies that translation of the newly formed mRNAs took at least 35 min. Translation is a particularly energy-demanding cellular process (51). Therefore, translation of the highly abundant glycolytic proteins may be strongly affected by the cellular energy status. The experimental system used in this study is well suited for studying the relationship between ATP status and induction of glycolytic proteins, e.g., by additional studies under aerobic conditions or by increasing the ATP demand by adding a weak acid, such as benzoate (8, 20, 53).

After the initial decrease in the rate of ATP production, the energy charge of the cells was gradually restored as a result of the increasing glycolytic flux. After 2 h, the q_{ATP} was twofold higher than that under the steady-state conditions that preceded the perturbation. Y_{ATP} calculations suggested that not all the additionally formed ATP was used for biomass formation. This apparent partial uncoupling of sugar dissimilation and assimilation suggests that there is activity of as-yet-unidentified free energy-requiring processes, such as protein turnover or heat production (35). The relatively inefficient sugar metabolism during glucose-excess conditions is consistent with an evolutionary strategy that is aimed at rapidly monopolizing sugars and creating an unfavorable environment for competitive microorganisms by rapid excretion of fermentation products.

The initial induction of fermentative capacity is regulated by metabolites. Qualitatively, the changes in intracellular metabolite levels that were measured during the initial phase of the switch to fermentative conditions were consistent with the notion that these changes contributed to the observed increase in the glycolytic flux. For example, the observed decrease in the intracellular trehalose-6-phosphate concentration was consistent with a gradual release of the inhibition of HXK by this metabolite (4). Similarly, the metabolite profiles for fructose-2,6-bisphosphate and fructose-1,6-bisphosphate are likely to have contributed to the activation of PFK and PYK, respectively (3, 25).

Attempts to quantitatively correlate the observed changes in metabolite levels with the measured glycolytic fluxes, with the aid of detailed kinetic equations for the individual glycolytic enzymes, were only partially successful. For four enzymes for which the known relevant metabolites were measured (PGI, PFK, PYK, and PDC), available published kinetic equations could not precisely fit the in vivo fluxes. In particular, the flux through PFK could not be described by a highly detailed kinetic model including activation by ADP, AMP, and fructose-2,6-bisphosphate and inhibition by ATP (39). Even fitting the in vitro-determined parameters did not improve the fit of the PFK kinetic equation, which strongly suggests that additional, as-yet-unknown effectors are involved in the in vivo regulation of PFK. The kinetic equations for PGI, PYK, and PDC could accurately describe the increase in flux after the perturbation when the corresponding kinetic parameters were fitted to the data. However, parameter sensitivity analysis revealed that the current data set did not allow precise determination of the individual kinetic parameters of these enzymes. The inability to identify parameters is a known, largely unresolved problem in in vivo pathway kinetics studies. Besides technical difficulties related to obtaining high-quality in vivo data, the information content of data obtained from in vivo experiments is constrained by the fact that metabolite concentrations change only within restricted physiological ranges and are often linked to concentrations of other metabolites. These restrictions do not arise in in vitro experiments, where a metabolite concentration can be changed at will. Improved experimental design and reduction of model complexity by approximative kinetics and model reduction (14) therefore remain key elements for in vivo pathway kinetics studies.

Quantitative regulation analysis confirmed two distinct phases in the fermentative response of *S. cerevisiae*. Regulation analysis (8, 34, 40) is a mathematical approach that enables quantification of the contribution of different levels of cellular regulation. It discriminates between hierarchical regulation

(regulation of enzyme capacity, primarily via protein synthesis and/or degradation) and metabolic regulation (modulation of enzyme activity, primarily via low-molecular-weight metabolites). Calculation of hierarchical and metabolic coefficients (see File S2 in the supplemental material) confirmed that in the first 45 min after the switch to fermentative conditions, regulation could be completely assigned to metabolic regulation. In the second phase (45 to 120 min), almost completely hierarchical regulation (which covers transcription, translation, and posttranslational modification) was observed for the enzymes PGI, FBA, TPI, GAPDH, GPM, ENO, PYK, and PDC. The remaining four enzymes, HXK, PFK, PGK, and ADH, were completely governed by metabolic regulation during the entire experiment. Recent studies of steady-state cultures have pioneered the use of regulation analysis for dissecting hierarchical regulation into transcriptional, translational, and posttranslational regulation (8). Application of such a high-information-density, multilevel, systems biology approach to the dynamic situation described in the present study should contribute to a deeper understanding of the mechanisms of glycolytic regulation in *S. cerevisiae*.

APPENDIX

Kinetic equations. The reversible reaction catalyzed by PGI was described by one-substrate, one-product reversible Michaelis-Menten kinetics (41):

$$v = V_{\max}\frac{\frac{[\mathrm{G6P}]}{K_{\mathrm{G6P}}}\left(1-\frac{\Gamma}{K_{\mathrm{eq}}}\right)}{1+\frac{[\mathrm{G6P}]}{K_{\mathrm{G6P}}}+\frac{[\mathrm{F6P}]}{K_{\mathrm{F6P}}}} \quad (2)$$

where v is the flux, $V_{\max}$ is the maximal rate, [G6P] is the concentration of glucose-6-phosphate, [F6P] is the concentration of fructose-6-phosphate, Γ is the mass-action ratio ([F6P]/[G6P]), K_{eq} is the equilibrium constant, and K_{G6P} and K_{F6P} are the Michaelis-Menten constants for glucose-6-phosphate and fructose-6-phosphate, respectively.

The kinetic model used for PFK was a function of the concentrations of fructose-6-phosphate, ATP ([ATP]), AMP ([AMP]), fructose-2,6-bisphosphate ([F26bP]), and fructose-1,6-bisphosphate ([F16bP]). All the effects were captured in one rate equation, as described by Teusink et al. (41):

$$v = V_{\max}\frac{g_R\lambda_1\lambda_2 R}{R^2+\mathrm{LT}^2} \quad (3)$$

with

$$\lambda_1 = [\mathrm{F6P}]/K_{R,\mathrm{F6P}}, \quad \lambda_1 = [\mathrm{ATP}]/K_{R,\mathrm{ATP}} \quad (4a,b)$$

$$R = 1+\lambda_1\lambda_2+g_R\lambda_1\lambda_2, \quad T = 1+c_{\mathrm{ATP}}\lambda_2 \quad (5a,b)$$

$$L = L_0\left(\frac{1+C_{i,\mathrm{ATP}}[\mathrm{ATP}]/K_{\mathrm{ATP}}}{1+[\mathrm{ATP}]/K_{\mathrm{ATP}}}\right)^2\cdot\left(\frac{1+C_{i,\mathrm{AMP}}[\mathrm{AMP}]/K_{\mathrm{AMP}}}{1+[\mathrm{AMP}]/K_{\mathrm{AMP}}}\right)^2\cdot \left(\frac{1+C_{i,\mathrm{F26bP}}[\mathrm{F26bP}]/K_{\mathrm{F26bP}}+C_{i,\mathrm{F16bP}}[\mathrm{F16bP}]/K_{\mathrm{F16bP}}}{1+[\mathrm{F26bP}]/K_{\mathrm{F26bP}}+[\mathrm{F16bP}]/K_{\mathrm{F16bP}}}\right) \quad (6)$$

where L_O is the allosteric constant, K_{ATP}, K_{AMP}, K_{F26bP}, and K_{F16bP} are the constants for ATP, AMP, fructose-2,6-bisphosphate, and fructose-1,6-bisphosphate, respectively, and $C_{i,\mathrm{ATP}}$ $C_{i,\mathrm{AMP}}$, $C_{i,\mathrm{F26bP}}$, and $C_{i,\mathrm{F16bP}}$ are the inhibition concentrations of ATP, AMP, fructose-2,6-bisphosphate, and fructose-1,6-bisphosphate, respectively.

For the enzyme PYK two different kinetic equations were used, with and without activation by fructose-1,6-bisphosphate. The kinetics without an activator were described by Michaelis-Menten kinetics for two noncompeting substrate-product couples (41):

$$v = V_{\max}\frac{\frac{[\mathrm{PEP}][\mathrm{ADP}]}{K_{\mathrm{PEP}}K_{\mathrm{ADP}}}\left(1-\frac{\Gamma}{K_{\mathrm{eq}}}\right)}{\left(1+\frac{[\mathrm{PEP}]}{K_{\mathrm{PEP}}}+\frac{[\mathrm{Pyr}]}{K_{\mathrm{Pyr}}}\right)\left(1+\frac{[\mathrm{ADP}]}{K_{\mathrm{ADP}}}+\frac{[\mathrm{ATP}]}{K_{\mathrm{ATP}}}\right)} \quad (7)$$

where [PEP] and [ADP] are the concentrations of phosphoenolpyruvate (PEP) and ADP, respectively, [Pyr] and [ATP] are the concentrations of the products pyruvate and ATP, respectively, Γ is the mass-action ratio, and K_{PEP}, K_{ADP}, K_{Pyr}, and K_{ATP} are the constants for phosphoenolpyruvate, ADP, pyruvate, and ATP. The equation of Rizzi et al. (32) included the activation by fructose-1,6-bisphosphate:

$$v = V_{\max}\frac{\frac{[\mathrm{PEP}]}{K_{\mathrm{PEP}}}\left(\frac{[\mathrm{PEP}]}{K_{\mathrm{PEP}}}+1\right)^{n-1}}{L_0\left(\frac{[\mathrm{ATP}]}{K_{\mathrm{ATP}}}+1\Big/\frac{[\mathrm{FbP}]}{K_{\mathrm{FbP}}}\right)+1\Big)^n\left(1+\frac{[\mathrm{PEP}]}{K_{\mathrm{PEP}}}\right)^n}\cdot \frac{[\mathrm{ADP}]}{[\mathrm{ADP}]+K_{\mathrm{ADP}}} \quad (8)$$

where [FbP] is the concentration of fructose-1,6-bisphosphate, K_{FbP} is the Michaelis-Menten constant for fructose-1,6-bisphosphate, L_O is the allosteric constant, and n is the interaction factor for subunits.

The reaction catalyzed by PDC was described by irreversible Hill kinetics, as described by Teusink et al. (41):.

$$v = V_{\max}\frac{\left(\frac{[\mathrm{Pyr}]}{K_{\mathrm{Pyr}}}\right)^{n_{\mathrm{H}}}}{1+\left(\frac{[\mathrm{Pyr}]}{K_{\mathrm{Pyr}}}\right)^{n_{\mathrm{H}}}} \quad (9)$$

where [Pyr] is the pyruvate concentration, K_{Pyr} is the constant for pyruvate, and n_H is the Hill coefficient. The parameters used in all kinetic equations are shown in Tables 1 and 2.

ACKNOWLEDGMENTS

We thank Johan Knoll, Jan van Dam, Reza Maleki Seifar, and Angela ten Pierick for technical assistance with measuring the intracellular metabolites.

This project was financially supported by the IOP Genomics Program of Senter Novem, The Netherlands.

REFERENCES

1. **Adams, B. G.** 1972. Induction of galactokinase in *Saccharomyces cerevisiae*: kinetics of induction and glucose effects. J. Bacteriol. **111:**308–315.
2. **Atkinson, D. E.** 1968. The energy charge of the adenylate pool as a regulatory parameter. Interaction with feedback modifiers. Biochemistry **7:**4030–4034.
3. **Bartrons, R., E. Van Schaftingen, S. Vissers, and H. G. Hers.** 1982. The stimulation of yeast phosphofructokinase by fructose 2,6-bisphosphate. FEBS Lett. **143:**137–140.

4. **Blazquez, M. A., R. Lagunas, C. Gancedo, and J. M. Gancedo.** 1993. Trehalose-6-phosphate, a new regulator of yeast glycolysis that inhibits hexokinases. FEBS Lett. **329:**51–54.
5. **Camarasa, C., J. P. Grivet, and S. Dequin.** 2003. Investigation by ^{13}C-NMR and tricarboxylic acid (TCA) deletion mutant analysis of pathways for succinate formation in *Saccharomyces cerevisiae* during anaerobic fermentation. Microbiology **149:**2669–2678.
6. **Canelas, A. B., W. M. van Gulik, and J. J. Heijnen.** 2008. Determination of the cytosolic free NAD/NADH ratio in *Saccharomyces cerevisiae* under steady-state and highly dynamic conditions. Biotechnol. Bioeng. **100:**734–743.
7. **Daran-Lapujade, P., M. L. A. Jansen, J. M. Daran, W. van Gulik, J. H. de Winde, and J. T. Pronk.** 2004. Role of transcriptional regulation in controlling fluxes in central carbon metabolism of *Saccharomyces cerevisiae*—a chemostat culture study. J. Biol. Chem. **279:**9125–9138.
8. **Daran-Lapujade, P., S. Rossell, W. van Gulik, M. A. Luttik, M. J. L. de Groot, M. Slijper, A. J. Heck, J. M. Daran, J. H. de Winde, H. V. Westerhoff, J. T. Pronk, and B. M. Bakker.** 2007. The fluxes through glycolytic enzymes in *Saccharomyces cerevisiae* are predominantly regulated at posttranscriptional levels. Proc. Natl. Acad. Sci. USA **104:**15753–15758.
9. **Ferea, T. L., D. Botstein, P. O. Brown, and R. F. Rosenzweig.** 1999. Systematic changes in gene expression patterns following adaptive evolution in yeast. Proc. Natl. Acad. Sci. USA **96:**9721–9726.
10. **Flikweert, M. T., M. Kuyper, A. J. van Maris, P. Kotter, J. P. van Dijken, and J. T. Pronk.** 1999. Steady-state and transient-state analysis of growth and metabolite production in a *Saccharomyces cerevisiae* strain with reduced pyruvate-decarboxylase activity. Biotechnol. Bioeng. **66:**42–50.
11. **Francois, J., and J. L. Parrou.** 2001. Reserve carbohydrates metabolism in the yeast *Saccharomyces cerevisiae*. FEMS Microbiol. Rev. **25:**125–145.
12. **Gancedo, J. M.** 1998. Yeast carbon catabolite repression. Microbiol. Mol. Biol. Rev. **62:**334–361.
13. **Gombert, A. K., M. M. dos Santos, B. Christensen, and J. Nielsen.** 2001. Network identification and flux quantification in the central metabolism of *Saccharomyces cerevisiae* under different conditions of glucose repression. J. Bacteriol. **183:**1441–1451.
14. **Heijnen, J. J.** 2005. Approximative kinetic formats used in metabolic network modeling. Biotechnol. Bioeng. **91:**534–545.
15. **Hubner, G., R. Weidhase, and A. Schellenberger.** 1978. The mechanism of substrate activation of pyruvate decarboxylase: a first approach. Eur. J. Biochem. **92:**175–181.
16. **Jansen, M. L., P. Daran-Lapujade, J. H. de Winde, M. D. Piper, and J. T. Pronk.** 2004. Prolonged maltose-limited cultivation of *Saccharomyces cerevisiae* selects for cells with improved maltose affinity and hypersensitivity. Appl. Environ. Microbiol. **70:**1956–1963.
17. **Jansen, M. L., J. A. Diderich, M. Mashego, A. Hassane, J. H. de Winde, P. Daran-Lapujade, and J. T. Pronk.** 2005. Prolonged selection in aerobic, glucose-limited chemostat cultures of *Saccharomyces cerevisiae* causes a partial loss of glycolytic capacity. Microbiology **151:**1657–1669.
18. **Kleijn, R. J., W. A. van Winden, C. Ras, W. M. van Gulik, D. Schipper, and J. J. Heijnen.** 2006. ^{13}C-labeled gluconate tracing as a direct and accurate method for determining the pentose phosphate pathway split ratio in *Penicillium chrysogenum*. Appl. Environ. Microbiol. **72:**4743–4754.
19. **Kresnowati, M. T. A. P., W. A. van Winden, M. J. Almering, A. ten Pierick, C. Ras, T. A. Knijnenburg, P. Daran-Lapujade, J. T. Pronk, J. J. Heijnen, and J. M. Daran.** 2006. When transcriptome meets metabolome: fast cellular responses of yeast to sudden relief of glucose limitation. Mol. Syst. Biol. **2:**49.
20. **Kresnowati, M. T. A. P., C. Suarez-Mendez, M. K. Groothuizen, W. A. van Winden, and J. J. Heijnen.** 2007. Measurement of fast dynamic intracellular pH in *Saccharomyces cerevisiae*, using benzoic acid pulse. Biotechnol. Bioeng. **97:**86–98.
21. **Lagunas, R.** 1976. Energy metabolism of *Saccharomyces cerevisiae* discrepancy between ATP balance and known metabolic functions. Biochim. Biophys. Acta **440:**661–674.
22. **Lange, H. C., M. Eman, G. van Zuijlen, D. Visser, J. C. van Dam, J. Frank, M. J. de Mattos, and J. J. Heijnen.** 2001. Improved rapid sampling for in vivo kinetics of intracellular metabolites in *Saccharomyces cerevisiae*. Biotechnol. Bioeng. **75:**406–415.
23. **Lowry, O. H., N. J. Rosebrough, A. L. Farr, and R. J. Randall.** 1951. Protein measurement with the Folin phenol reagent. J. Biol. Chem. **193:**265–275.
24. **Mashego, M. R., M. L. Jansen, J. L. Vinke, W. M. van Gulik, and J. J. Heijnen.** 2005. Changes in the metabolome of *Saccharomyces cerevisiae* associated with evolution in aerobic glucose-limited chemostats. FEMS Yeast Res. **5:**419–430.
25. **Murcott, T. H., H. Gutfreund, and H. Muirhead.** 1992. The cooperative binding of fructose-1,6-bisphosphate to yeast pyruvate kinase. EMBO J. **11:**3811–3814.
26. **Pahlman, A. K., K. Granath, R. Ansell, S. Hohmann, and L. Adler.** 2001. The yeast glycerol 3-phosphatases gpp1p and gpp2p are required for glycerol biosynthesis and differentially involved in the cellular responses to osmotic, anaerobic, and oxidative stress. J. Biol. Chem. **276:**3555–3563.
27. **Parrou, J. L., and J. Francois.** 1997. A simplified procedure for a rapid and reliable assay of both glycogen and trehalose in whole yeast cells. Anal. Biochem. **248:**186–188.
28. **Portela, P., S. Howell, S. Moreno, and S. Rossi.** 2002. In vivo and in vitro phosphorylation of two isoforms of yeast pyruvate kinase by protein kinase A. J. Biol. Chem. **277:**30477–30487.
29. **Postma, E., A. Kuiper, W. F. Tomasouw, W. A. Scheffers, and J. P. van Dijken.** 1989. Competition for glucose between the yeasts *Saccharomyces cerevisiae* and *Candida utilis*. Appl. Environ. Microbiol. **55:**3214–3220.
30. **Pronk, J. T., H. Yde Steensma, and J. P. van Dijken.** 1996. Pyruvate metabolism in *Saccharomyces cerevisiae*. Yeast **12:**1607–1633.
31. **Richter, O., A. Betz, and C. Giersch.** 1975. The response of oscillating glycolysis to perturbations in the NADH/NAD system: a comparison between experiments and a computer model. Biosystems **7:**137–146.
32. **Rizzi, M., M. Baltes, U. Theobald, and M. Reuss.** 2000. In vivo analysis of metabolic dynamics in *Saccharomyces cerevisiae*. II. Mathematical model. Biotechnol. Bioeng. **55:**592–608.
33. **Rossell, S., C. C. van der Weijden, A. Kruckeberg, B. M. Bakker, and H. V. Westerhoff.** 2002. Loss of fermentative capacity in baker's yeast can partly be explained by reduced glucose uptake capacity. Mol. Biol. Rep. **29:**255–257.
34. **Rossell, S., C. C. van der Weijden, A. Lindenbergh, A. van Tuijl, C. Francke, B. M. Bakker, and H. V. Westerhoff.** 2006. Unraveling the complexity of flux regulation: a new method demonstrated for nutrient starvation in *Saccharomyces cerevisiae*. Proc. Natl. Acad. Sci. USA **103:**2166–2171.
35. **Russell, J. B.** 2007. The energy spilling reactions of bacteria and other organisms. J. Mol. Microbiol. Biotechnol. **13:**1–11.
36. **Sierkstra, L. N., J. M. Verbakel, and C. T. Verrips.** 1992. Analysis of transcription and translation of glycolytic enzymes in glucose-limited continuous cultures of *Saccharomyces cerevisiae*. J. Gen. Microbiol. **138:**2559–2566.
37. **Stephanopoulos, G. N., A. A. Aristidou, and J. Nielsen.** 1998. Metabolic engineering. Principles and methodologies. Elsevier Science (USA), New York, NY.
38. **Stuckrath, I., H. C. Lange, P. Kotter, W. M. van Gulik, K. D. Entian, and J. J. Heijnen.** 2002. Characterization of null mutants of the glyoxylate cycle and gluconeogenic enzymes in *S. cerevisiae* through metabolic network modeling verified by chemostat cultivation. Biotechnol. Bioeng. **77:**61–72.
39. **Tai, S. L., P. Daran-Lapujade, M. A. Luttik, M. C. Walsh, J. A. Diderich, G. C. Krijger, W. M. van Gulik, J. T. Pronk, and J. M. Daran.** 2007. Control of the glycolytic flux in *Saccharomyces cerevisiae* grown at low temperature: a multi-level analysis in anaerobic chemostat cultures. J. Biol. Chem. **282:**10243–10251.
40. **ter Kuile, B. H., and H. V. Westerhoff.** 2001. Transcriptome meets metabolome: hierarchical and metabolic regulation of the glycolytic pathway. FEBS Lett. **500:**169–171.
41. **Teusink, B., J. Passarge, C. A. Reijenga, E. Esgalhado, C. C. van der Weijden, M. Schepper, M. C. Walsh, B. M. Bakker, K. van Dam, H. V. Westerhoff, and J. L. Snoep.** 2000. Can yeast glycolysis be understood in terms of in vitro kinetics of the constituent enzymes? Testing biochemistry. Eur. J. Biochem. **267:**5313–5329.
42. **Theobald, U., W. Mailinger, M. Baltes, M. Rizzi, and M. Reuss.** 2000. In vivo analysis of metabolic dynamics in *Saccharomyces cerevisiae*. I. Experimental observations. Biotechnol. Bioeng. **55:**305–316.
43. **van Dam, J. C., M. R. Eman, J. Frank, H. C. Lange, G. W. K. van Dedem, and J. J. Heijnen.** 2002. Analysis of glycolytic intermediates in *Saccharomyces cerevisiae* using anion exchange chromatography and electrospray ionization with tandem mass spectrometric detection. Anal. Chim. Acta **460:**209–218.
44. **van den Berg, M. A., P. Jong-Gubbels, C. J. Kortland, J. P. van Dijken, J. T. Pronk, and H. Y. Steensma.** 1996. The two acetyl-coenzyme A synthetases of *Saccharomyces cerevisiae* differ with respect to kinetic properties and transcriptional regulation. J. Biol. Chem. **271:**28953–28959.
45. **van den Brink, J., P. Daran-Lapujade, J. T. Pronk, and J. H. de Winde.** 2008. New insights into the *Saccharomyces cerevisiae* fermentation switch: dynamic transcriptional response to anaerobicity and glucose-excess. BMC Genomics **9:**100.
46. **van Dijken, J. P., J. Bauer, L. Brambilla, P. Duboc, J. M. Francois, C. Gancedo, M. L. Giuseppin, J. J. Heijnen, M. Hoare, H. C. Lange, E. A. Madden, P. Niederberger, J. Nielsen, J. L. Parrou, T. Petit, D. Porro, M. Reuss, N. van Riel, M. Rizzi, H. Y. Steensma, C. T. Verrips, J. Vindelov, and J. T. Pronk.** 2000. An interlaboratory comparison of physiological and genetic properties of four *Saccharomyces cerevisiae* strains. Enzyme Microb. Technol. **26:**706–714.
47. **van Dijken, J. P., R. A. Weusthuis, and J. T. Pronk.** 1993. Kinetics of growth and sugar consumption in yeasts. Antonie van Leeuwenhoek **63:**343–352.
48. **van Hoek, P., J. P. van Dijken, and J. T. Pronk.** 1998. Effect of specific growth rate on fermentative capacity of baker's yeast. Appl. Environ. Microbiol. **64:**4226–4233.
49. **van Hoek, P., J. P. van Dijken, and J. T. Pronk.** 2000. Regulation of fermentative capacity and levels of glycolytic enzymes in chemostat cultures of *Saccharomyces cerevisiae*. Enzyme Microb. Technol. **26:**724–736.
50. **Van Urk, H., P. R. Mak, W. A. Scheffers, and J. P. van Dijken.** 1988. Metabolic responses of *Saccharomyces cerevisiae* CBS 8066 and *Candida utilis* CBS 621 upon transition from glucose limitation to glucose excess. Yeast **4:**283–291.

51. **Verduyn, C., E. Postma, W. A. Scheffers, and J. P. van Dijken.** 1990. Energetics of *Saccharomyces cerevisiae* in anaerobic glucose-limited chemostat cultures. J. Gen. Microbiol. **136:**405–412.
52. **Verduyn, C., E. Postma, W. A. Scheffers, and J. P. van Dijken.** 1990. Physiology of *Saccharomyces cerevisiae* in anaerobic glucose-limited chemostat cultures. J. Gen. Microbiol. **136:**395–403.
53. **Verduyn, C., E. Postma, W. A. Scheffers, and J. P. van Dijken.** 1992. Effect of benzoic acid on metabolic fluxes in yeasts: a continuous-culture study on the regulation of respiration and alcoholic fermentation. Yeast **8:**501–517.
54. **Verduyn, C., A. H. Stouthamer, W. A. Scheffers, and J. P. van Dijken.** 1991. A theoretical evaluation of growth yields of yeasts. Antonie van Leeuwenhoek **59:**49–63.
55. **Visser, D., G. A. van Zuylen, J. C. van Dam, M. R. Eman, A. Proll, C. Ras, L. Wu, W. M. van Gulik, and J. J. Heijnen.** 2004. Analysis of in vivo kinetics of glycolysis in aerobic *Saccharomyces cerevisiae* by application of glucose and ethanol pulses. Biotechnol. Bioeng. **88:**157–167.
56. **Visser, W., W. A. Scheffers, W. H. Batenburg-van der Vegte, and J. P. van Dijken.** 1990. Oxygen requirements of yeasts. Appl. Environ. Microbiol. **56:**3785–3792.
57. **Wu, L., M. R. Mashego, J. C. van Dam, A. M. Proell, J. L. Vinke, C. Ras, W. A. van Winden, W. M. van Gulik, and J. J. Heijnen.** 2005. Quantitative analysis of the microbial metabolome by isotope dilution mass spectrometry using uniformly ^{13}C-labeled cell extracts as internal standards. Anal. Biochem. **336:**164–171.